Global Conformation of a Self-Cleaving Hammerhead RNA†

Khaled M. A. Amiri and Paul J. Hagerman*

Department of Biochemistry, Biophysics and Genetics, University of Colorado Health Sciences Center, Denver, Colorado 80262

Received July 22, 1994; Revised Manuscript Received September 20, 1994®

ABSTRACT: Phylogenetic and biochemical studies of RNA have provided a wealth of information regarding secondary structure; however, knowledge of tertiary structure has been more difficult to obtain. In the current work, electrophoretic and hydrodynamic measurements have yielded the global conformations of a self-cleaving "hammerhead" RNA, both prior to and following self-cleavage. The pre- and post-cleavage structures appear to have nearly identical conformations in which the three helices assume a roughly coplanar arrangement with well-defined interhelix angles. Following self-cleavage, one of the three helix stems (stem I) undergoes a slight (<10°) realignment, although the relative positions of the other two stems remain unchanged. Extension of stem III from (nominally) three base pairs to nine base pairs, known to dramatically enhance the rate of self-cleavage, results in a substantial (~70°) realignment of stems I and II. The current study represents an approach for studying other nonhelical elements in RNA.

Interest in self-cleaving and catalytically active RNA molecules has grown rapidly since their discovery in the early 1980s (Cech, 1990; Altman et al., 1993), and the list of such species is expanding rapidly (Symons, 1991). One well-characterized system is the small, self-cleaving "hammerhead" RNA domain found in a number of plant viral-like pathogens (Symons, 1989, 1992). The RNA genomes of these pathogens are in the neighborhood of 400 nucleotides in length, and each contains a small, conserved region comprising nine unpaired bases and four paired bases that is necessary for the processing, *via* self-cleavage, of multimeric RNA replication intermediates (Hutchins et al., 1986; Forster and Symons, 1987; Robertson & Branch, 1987). Self-cleavage is effected through a transesterification reaction, mediated by various divalent cations, to yield 2′,3′-cyclic phosphate and 5′-hydroxyl termini (Symons, 1989; Hutchins et al., 1986). Although the hammerhead element is providing a wealth of information on the thermodynamics and kinetics of self-cleavage (Uhlenbeck, 1987; Fedor & Uhlenbeck, 1992; Hertel et al., 1994; Ruffner et al., 1989), information pertaining to the global conformation of the hammerhead remains sparse and is limited to NMR evidence for the presence of base-paired stems (Heus & Pardi, 1991; Heus et al., 1990; Odai et al., 1990; Pease & Wemmer, 1990).

We recently reported (Gast et al., 1994) a partial conformation for the hammerhead core, depicted in Figure 1A, which has been studied extensively by Uhlenbeck and coworkers (Uhlenbeck, 1987; Fedor & Uhlenbeck, 1992; Hertel et al., 1994; Ruffner et al., 1989). The approach used in the previous study involved a combination of gel electrophoretic and transient electric birefringence (TEB) (rotational diffusion) measurements of a modified hammerhead in which stems I and II were each extended by approximately 70 base pairs (bp) (modified version designated E[HH]; Gast et al., 1994).

The TEB experiments, which exploit the extreme sensitivity of birefringence decay times to the angles between pairs of extended helices, allowed Gast et al. (1994) to conclude that, for that extended hammerhead, helical stems I and II (Figure 1A) were essentially coaxial. The E[HH] construct used in that study is active in self-cleavage; however, its *rate* of cleavage is substantially slower (≥10-fold) than the rates reported for the hammerheads themselves (Uhlenbeck, 1987; Slim & Gait, 1991; Koizumi & Ohtsuka, 1991). There were at least two possible explanations for the observed difference in rates: (i) the elongated stems I and II were somehow inhibiting the cleavage reaction, or (ii) there was an intrinsic problem with the core structure of the hammerhead as depicted in Figure 1A. With regard to the latter, it has been suggested that a dimeric form of the hammerhead is an important intermediate in the normal cleavage reaction (Forster et al., 1988; Davies et al., 1991), although this suggestion has been questioned (Ruffner et al., 1989; see below). By design, the E[HH] structures are incapable of forming the dimeric hammerhead core structure and can be purified as a single band on gels. Therefore, E[HH] may reflect the intrinsic rates of cleavage of the single hammerhead species depicted in Figure 1A.

In the current work, all three pairwise-extended hammerhead species have been constructed in an effort to completely define the interhelix conformation of the hammerhead domain (Figure 1B). Each of the three constructs is fully active in self-cleavage, and their electrophoretic and hydrodynamic behavior is indicative of a well-formed conformation in which all three helices are essentially coplanar.

MATERIALS AND METHODS

Synthesis and Purification of DNA Oligonucleotides Used in Cloning. DNA oligonucleotides were synthesized on a Milligen/Biosearch 8750 automated DNA synthesizer, using

† This work was supported by a grant from the National Institutes of Health (P.J.H., GM 35305), and by a graduate fellowship (K.M.A.A.) from the United Arab Emirates University. Research in the laboratory is supported in part by a grant from the Lucille P. Markey Charitable Trust and by the University of Colorado Cancer Center Core Grant CA 46934-06 for the Oligonucleotide Synthesis Core Facility.

* Please address correspondence to this author at the Department of Biochemistry, Biophysics and Genetics, B-121, University of Colorado Health Sciences Center, 4200 E. 9th Ave., Denver, CO 80262. Ph: (303) 270-8305; FAX: (303) 270−5467.

® Abstract published in *Advance ACS Abstracts,* October 15, 1994.

0006-2960/94/0433-13172$04.50/0

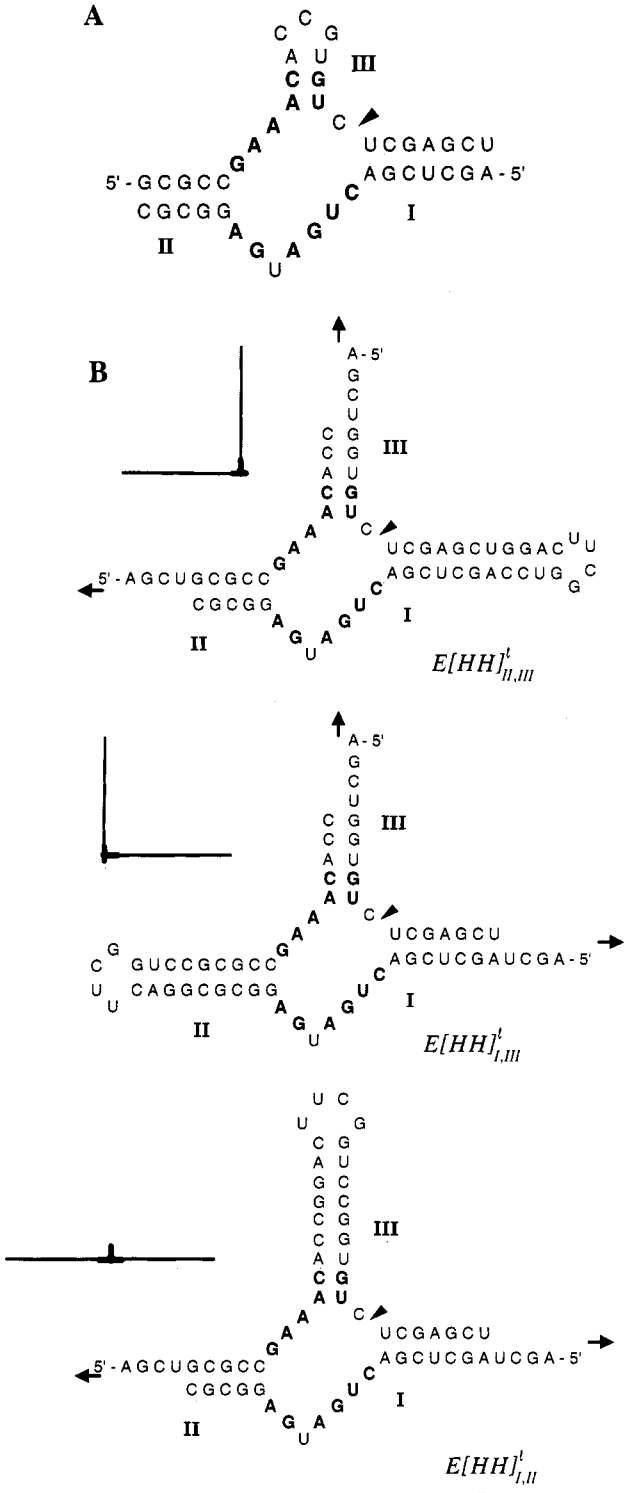

FIGURE 1: (A) The core structure for the self-cleaving hammerhead RNA (Uhlenbeck, 1987; Ruffner et al., 1989; Davies et al., 1991). The site of cleavage is indicated by a solid triangle. Conserved nucleotides are indicated in bold. (B) Extended hammerhead ($E[HH]^t_{i,j}$) constructs used in the current investigation. Each of the three heteroduplex constructs is formed by annealing two RNA transcripts such that pairs of helix stems are elongated to *ca.* 70 bp (per stem). The nonextended branches comprise stems of 9 bp ($E[HH]^t_{I,II}$], $E[HH]^t_{I,III}$) or 11 bp ($E[HH]^t_{II,III}$), each capped by a UUCG tetraloop. Thus, a construct in which stems I and II are extended, and in which the nonextended stem is 9 bp, is designated $E[HH]^t_{I,II}$. The $E[HH]^t_{i,j}$ constructs have been designed to exploit the sensitivity of gel electrophoresis and rotational diffusion measurements to the angles subtended by the extended stems.

β-cyanoethyl phosphoramidite chemistry. Synthesis reagents were purchased from Milligen/Biosearch. Methods employed for the purification and annealing of the DNA oligomers are essentially identical to those described elsewhere (Gast & Hagerman, 1991).

Production of the RNA Heteroduplex Molecules Representing the Extended Hammerhead Molecules. DNA oligomers corresponding to the hammerhead core were cloned into a central *Hin*dIII site of a pair of standard templates, essentially as described previously (Gast & Hagerman, 1991; Gast et al., 1994); however, the previous studies utilized pBR plasmid derivatives (pFU3A,B). The plasmids employed in the current study possess the same templates as those contained in the pFU plasmids; however, the templates have been transferred to pGEM-derivative plasmids for improved plasmid yield. The current (parent) plasmids are designated pGJ122A and pGJ122B, where the A(B) designation refers to the orientation of the template with respect to the T7 promoter as specified earlier (Gast et al., 1994). The transcripts from these two plasmids (*Sma*I linearized) are each 136 nt in the absence of inserts at the central *Hin*dIII site. When annealed, the fully-complementary transcripts yield a 136 bp RNA helix. The sequences of the *non*template strands of the inserts are as indicated in Figure 1B (represented as RNA sequence). Following cloning, selection, purification, and sequencing of the plasmids with inserts (Gast et al., 1994), transcription reactions were carried out according to the procedure of Milligan et al. (1987), with 2−4 mM of each of the four rNTPs and 50 nM *Sma*I-linearized plasmid for each reaction. The transcripts were passed through Sephadex G-25 (Pharmacia) columns that had been pre-equilibrated with MEEN buffer [100 mM 2-morpholinoethanesulfonic acid (MES), pH 5.5−6.0, 20 mM NaEDTA, 20 mM NaEGTA, and 100 mM NaCl]. Appropriate transcripts were annealed in MEEN buffer for 2 min at 95 °C, followed by slow cooling for *ca.* 20 minutes to 25 °C. The heteroduplex RNAs were purified from polyacrylamide gels and passed through Sephadex G-25 (Pharmacia) columns that had been pre-equilibrated with 10 mM MES, pH 6.0, and 1 mM NaEDTA. The RNA-containing eluent was stored frozen until further use. For the production of cleaved $E[HH]_{i,j}$ species for TEB and gel mobility measurements, the heteroduplex molecules were incubated in 100 mM Tris-HCl, 10 mM $MgCl_2$, pH 8.0, 20 °C for 1 h (≥95% cleaved) and were gel purified as above.

Determination of Relative Electrophoretic Mobilities and Analysis of the Cleavage Reactions. Methods used for the analysis of the electrophoretic behavior of the RNA heteroduplex species are essentially as described by Gast et al. (1994). Specific gel and/or self-cleavage reaction conditions were as specified in the legends to Figures 2 and 3. Relative electrophoretic mobilities were determined from the distances migrated by the $E[HH]_{i,j}$ species relative to the linear (159 bp) duplex RNA control.

Determination of the Interhelix Angles of the RNA Constructs Using Transient Electric Birefringence. Transient electric birefringence (TEB) measurements were performed essentially as described previously (Cooper & Hagerman, 1989; Gast & Hagerman, 1991; Gast et al., 1994; Shen & Hagerman, 1994). However, the instrument used for the current measurements is of a new design and incorporates a high-voltage pulse generator, a solid-state diode laser, a single-channel detector, and an 80 μL temperature-jacketed birefringence cell, all developed and built in the laboratory (Schleif and Hagerman, in preparation). The overall system response time is approximately 25 ns, based on the birefringence response of water. Details of the instrument will be

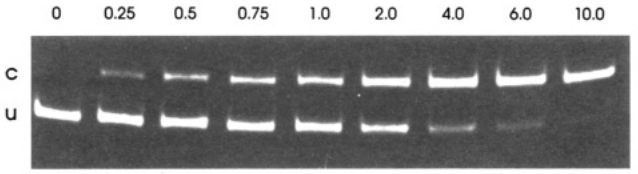

FIGURE 2: Video image of the time course of self-cleavage of E[HH]$'_{I,II}$. The cleavage reaction depicted in the image was performed in 100 mM Tris, pH 8.0, and 10 mM $MgCl_2$ at 25 °C. The reaction was initiated by the addition of $MgCl_2$. At specified time intervals, aliquots of the reaction mix were quenched with an equal volume of 50 mM NaEDTA, followed by storage at −20 °C. Times in minutes are indicated above each lane. Reaction products were analyzed on 6% polyacrylamide gels in running buffer (90 mM Tris-Borate, pH 7.4, 2.5 mM NaEDTA) lacking $MgCl_2$. The gels were recorded by video-imaging and were analyzed using ImageQuant software (Molecular Dynamics). The products of the cleavage reactions were verified on denaturing polyacrylamide/urea gels.

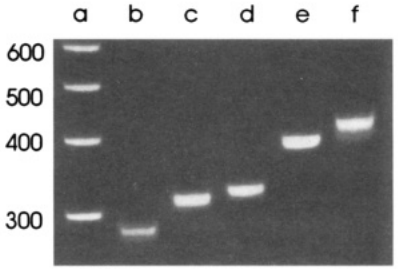

FIGURE 3: Electrophoretic mobilities of the extended hammerhead species, E[HH]$'_{i,j}$, employed in the current study. (Lane a) Control DNA ladder, with sizes in base pairs as indicated; (lane b) 159 bp linear duplex RNA; (lane c) E[HH]$^s_{I,II}$, studied previously (Gast et al., 1994); (lane d) E[HH]$'_{II,III}$; (lane e) E[HH]$'_{I,III}$; (lane f) E[HH]$'_{I,II}$. The gel depicted was run at 4 °C, with 10 mM $NaPO_4$ (pH 6.0) and 2 mM $MgCl_2$ as the running buffer. Buffer was continuously recirculated for all $NaPO_4$/Mg gels. The relative mobilities of all of the extended hammerhead species were nearly constant between pH 6 and 7.5 in the presence of Mg^{2+}. At the higher pH values, a small amount of self-cleavage occurs during the gel run.

presented elsewhere. The output of the detector was passed to a LeCroy Model 9310 digitizing oscilloscope. Disk files representing birefringence decay curves were transferred to 80486-based computers (Dell) for analysis. Following baseline subtraction and normalization, the decay curves were analyzed using laboratory software that incorporates the Levenberg−Marquardt (LM) method (Press et al., 1992), which has superseded the use of CONTIN (Provencher, 1982) in this laboratory. The LM method is also employed in the commercial software package, SigmaPlot (Jandel Scientific). The birefringence decay curves were, in all instances, well-represented by a two-exponential decay process, as observed previously (Cooper & Hagerman, 1989; Gast et al., 1994; Shen & Hagerman, 1994), and as anticipated from theory (Roitman, 1984; Roitman & Zimm, 1984a,b). The terminal (slowest) decay times were used for subsequent analysis of the interhelix angles (Hagerman & Zimm, 1981; Roitman, 1984; Roitman & Zimm, 1984a,b).

Interhelix angles were extracted from the terminal decay times, τ, for the E[HH]$_{i,j}$ species and the linear (159 bp) control molecule by comparing the experimental ratio, $\tau_{i,j}/\tau_{159}$, to the expected ratio, $\tau(\theta)/\tau(180°)$, for a given interhelix angle, θ. Plots of $\tau(\theta)/\tau(180°)$ as a function of θ were generated using the program DIFFROT, as described previously (Hagerman & Zimm, 1981; Cooper & Hagerman, 1989; Shen & Hagerman, 1994).

RNA molecules to be used for TEB measurements were passed through Sephadex G-25 columns (equilibrated with TEB buffer: 5 mM $NaPO_4$, 0.125 mM NaEDTA; $MgCl_2$, pH are as indicated in the table and figure legends) prior to being loaded into the TEB cell. TEB experiments typically utilized 5−20 μg of heteroduplex RNA for each set of measurements. Each set of measurements comprises five separate averages of 128−256 pulses (pulse width, 1 μs; repetition frequency 1 Hz; field strength 5−10 kV/cm). No sample degradation and no field strength dependence were noted for any samples in the current study.

RESULTS

Elongation of Stem III of E[HH] to 9 bp Results in More Than an Order of Magnitude Increase in the Rate of Self-Cleavage. In order to investigate the apparent discrepancy in the rates of self-cleavage between E[HH] (hereafter designated E[HH]$^s_{I,II}$; see: legend, Figure 1) and the nonextended hammerhead, stem III of E[HH]$^s_{I,II}$ has been extended from 3 to 9 bp (E[HH]$'_{I,II}$; Figure 1B). This extension results in a dramatic increase (≥100-fold) in the rates of self-cleavage (*e.g.*, Figure 2) to values that are in excess of 5 min^{-1} at pH 8, consistent with results for nonextended hammerheads (Fedor & Uhlenbeck, 1992). The current observation immediately rules out the first explanation for the apparent difference in rates: namely, that the elongated stems somehow interfere with self-cleavage within a single hammerhead. The second explanation, namely, that a single hammerhead with a 3 bp stem III is only moderately active in self-cleavage, remains viable. Previous studies with mutant hammerheads are consistent with the dimer hammerhead being the principal mode of cleavage for species with short stem III (Forster et al., 1988; Davies et al., 1991). Moreover, it is possible that the slow rates of cleavage observed by Ruffner et al. (1989) for mutant, dimeric hammerhead ribozymes may reflect an unfavorable equilibrium balance between (inactive) single hammerheads and partially active dimer hammerheads. Thus, for hammerheads with a short (and presumably only marginally stable) stem/loop III, cleavage may be more rapid in the dimer form; however, as the length of stem III increases, the cleavage rates for monomer and dimer species would be expected to approach one another. This latter issue will be discussed in more detail elsewhere (Amiri and Hagerman, unpublished experiments). However, ribonuclease probing experiments have also suggested that a short stem III is unstable (Hodgson et al., 1994).

The Elongation of Stem III Results in a Substantial Rearrangement of the Relative Orientations of Stems I and II. A striking feature of E[HH]$'_{I,II}$ is that the relative orientation of stems I and II is quite different from the essentially coaxial arrangement found in E[HH]$^s_{I,II}$. This interstem rearrangement can be appreciated by inspection of the gel pattern in Figure 3, where the mobility of E[HH]$'_{I,II}$ (lane f) is substantially reduced relative to that of E[HH]$^s_{I,II}$ (lane c). Since these mobilities primarily reflect the acuteness of the interstem angle for the pairs of elongated stems (Cooper & Hagerman, 1987) (by analogy with the gel behavior of curved DNA; Hagerman, 1990, 1992; Crothers et al., 1990), the gel behavior suggests that the interstem angle for E[HH]$'_{I,II}$ is much less than 180°. In fact, for the set of extended hammerhead species, E[HH]$'_{i,j}$, each with a 9 bp short stem, the angle between stems I and II appears to be much more acute than the angle subtended by stems II

Table 1: Relative Electrophoretic Mobilities for the Various Two-Helix Extensions of the Hammerhead Core

RNA species	μ_{ij}/μ_{159}[a] uncleaved	cleaved	ratio (uncleaved/cleaved)
$E[HH]^{\prime}_{II,III}$	0.88 ± 0.02	0.89 ± 0.00	0.99
$E[HH]^{\prime}_{I,III}$	0.75 ± 0.01	0.76 ± 0.02	0.99
$E[HH]^{\prime}_{I,II}$	0.70 ± 0.02	0.77 ± 0.02	0.91

[a] Relative electrophoretic mobilities in 6% polyacrylamide gels (2 mM $MgCl_2$, 10 mM $NaPO_4$, 0.125 mM NaEDTA, pH 7.0) run at 4 °C.

and III ($E[HH]^{\prime}_{II,III}$; lane d), and marginally more acute than the angle subtended by stems I and III ($E[HH]^{\prime}_{I,III}$; lane e). Furthermore, the small reduction in the mobility of $E[HH]^{\prime}_{II,III}$ compared to $E[HH]^{s}_{I,II}$; suggests that the former is slightly bent, although the increase in the length of stem III could contribute to this mobility difference. Finally, the data presented in Table 1 indicate that, in the presence of Mg^{2+} ions, there are no detectable differences in the relative mobilities of the cleaved and uncleaved forms of $E[HH]^{\prime}_{I,III}$ or $E[HH]^{\prime}_{II,III}$. However, the relative mobility of $E[HH]^{\prime}_{I,II}$ increases slightly upon cleavage.

Transient Electric Birefringence Measurements of the Three Extended Hammerhead RNAs Reveal an Essentially Planar Conformation of the Three Helices Bounding the Hammerhead Core, both Prior to and Following Self-Cleavage. In an effort to quantify the three angles defined by stems I, II, and III of the hammerhead core, thereby defining its overall conformation, each member of the $E[HH]^{\prime}_{i,j}$ set was subjected to analysis by transient electric birefringence (Figure 4) in a manner strictly analogous to the approach taken previously (Gast et al., 1994; Cooper & Hagerman, 1989; Gast & Hagerman, 1991). For each member of the set, the terminal (longer) birefringence decay time (Figure 4) was compared to the corresponding decay time for a pure duplex (159 bp) RNA control molecule, the ratio of the two decay times being a measure of the interstem angle (Gast et al., 1994; Cooper & Hagerman, 1989; Zacharias and Hagerman, unpublished experiments). The results of the current analysis are presented in Table 2 and Figure 5. Three features of the apparent angles in Table 2 are particularly significant. First, the angles sum to 360° within experimental error. This observation is important in that it suggests that the hammerhead core is nearly planar, and not particularly flexible. Second, the angle subtended by stems I and II has been reduced by ~70° as the length of stem III is increased from 3 to 9 bp. Thus, modification of a helix stem at a point that is somewhat removed from the catalytic center results in a substantial rearrangement of the conformation of the hammerhead. Although the functional relationship between this conformational shift and the observed increase in the rate of self-cleavage for elongated stem III has not been defined, they both may reflect a stabilization of the catalytic center as stem III becomes more stable. In this regard, it should be noted that further lengthening of stem III beyond 9 bp has essentially no effect on the rate of self-cleavage; in particular, the rates of self-cleavage for the three $E[HH]^{\prime}_{i,j}$ are all comparable (Amiri and Hagerman, unpublished experiments).

Third, the interstem angles of the cleaved hammerhead in the presence of Mg^{2+} ions are nearly identical to those of the uncleaved species, except for a slight (3−8°) realignment of stem I following cleavage (Table 2; Figures 4, and 5). These observations are consistent with the mobility data, which suggest a slight widening of the interhelix (I, II) angle upon cleavage (Table 1).

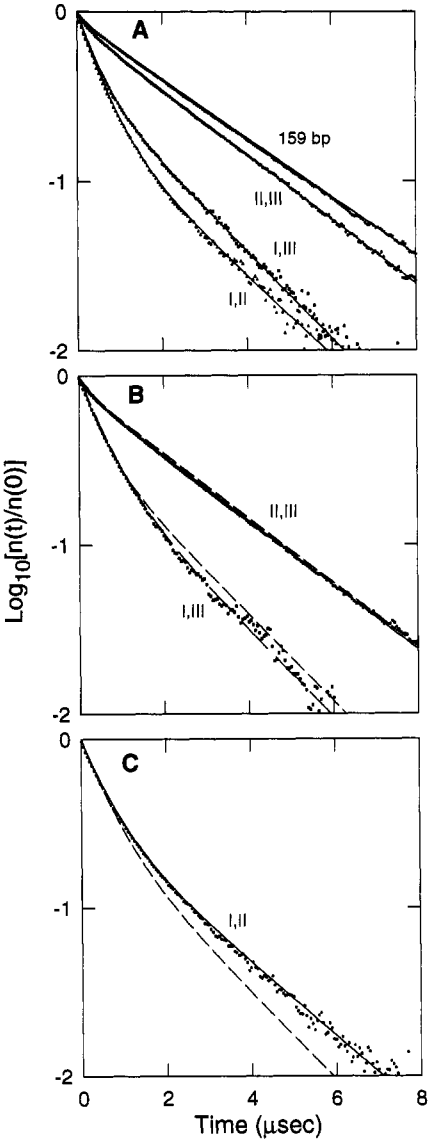

FIGURE 4: Semilog plots of the field-free decay of birefrigence for the RNA species used in the current investigations. (A) Decay profiles of all uncleaved RNA species (each species is indicated on the plot); (B) profiles for the cleaved species (solid line and symbols), $E[HH]^{\prime}_{II,III}$ and $E[HH]^{\prime}_{I,III}$; (C) profile for $E[HH]^{\prime}_{I,II}$. In (B) and (C), corresponding curves for the uncleaved species are represented as dashed lines for comparison. All lines (solid or dashed) represent double-exponential fits to the data using the LM method (see the Materials and Methods section). In the TEB experiments, the RNA molecules in an optical cell are partially oriented by a brief (1 μs), high-voltage pulse. The transient optical anisotropy of the solution alters the polarization characteristics of light passing through the cell, resulting in a temporary change in the amount of light that passes through a second polarizer. Following removal of the field, the normalized decay of the (birefringence) signal, $n(t)/n(0)$, is analyzed (Cooper & Hagerman, 1989; Gast & Hagerman, 1991); the terminal decay times for the extended hammerhead species are compared to the corresponding time for the linear control; the experimental ratios, $\tau_{E[HH]}/\tau_{159}$, are compared to computed $\tau_\theta/\tau_{linear}$ vs θ curves (see Materials and Methods). For the curves presented, the buffer was 5 mM $NaPO_4$, pH 6.0, and 2 mM $MgCl_2$, 3.6 °C. No differences in the decay times were observed for the RNA species between pH 6 and 7, nor were any differences observed as a function of field strength.

Table 2: Transient Electric Birefringence Results for the Extended Hammerhead Species, both Pre- and Post-Cleavage

RNA species	α^a	τ^a	$\tau_{i,j}/\tau_{159}$	angle^b (deg)
159 bp duplex	0.91 ± 0.02	2.60 ± 0.07		
uncleaved				
E[HH]$'_{II,III}$	0.79 ± 0.02	2.36 ± 0.05	0.90 ± 0.03	143 ± 6
E[HH]$'_{I,III}$	0.34 ± 0.05	1.92 ± 0.13	0.74 ± 0.05	116 ± 5
E[HH]$'_{I,II}$	0.26 ± 0.04	1.86 ± 0.19	0.72 ± 0.06	111 ± 8
cleaved				
E[HH]$'_{II,III,clv}$	0.81 ± 0.01	2.27 ± 0.01	0.91 ± 0.01	145 ± 2
E[HH]$'_{I,III,clv}$	0.30 ± 0.02	1.78 ± 0.08	0.71 ± 0.03	113 ± 3
E[HH]$'_{I,II,clv}$	0.36 ± 0.01	1.93 ± 0.04	0.77 ± 0.02	119 ± 3

^{a} α is the fractional amplitude associated with the terminal decay time, τ. ^{b} Apparent angles were determined by comparing the experimental $\tau_{i,j}/\tau_{159}$ ratios to the computed ratios, $\tau(\theta)/\tau(180°)$, as described in the text.

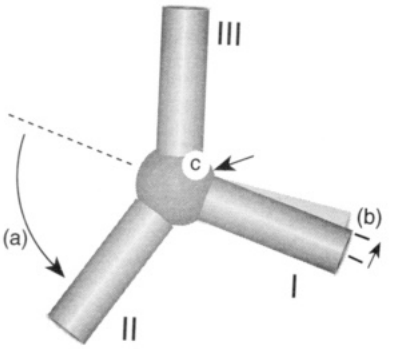

FIGURE 5: Cylinder representation of the spatial arrangement of the three helix stems bounding the hammerhead core. The arrow at "c" indicates the position of cleavage 3′ to the C residue (Figure 1A). (a) Conformational shift associated with extension of stem III to 9 bp in the presence of Mg^{2+}. (b) Shift in the position of stem I after cleavage.

DISCUSSION

The "apparent" designation for the derived angles in Table 2 stems from three sources of uncertainty. First, the linear dimensions of the nonpaired core region are not accurately known; therefore, the 159 bp control may slightly overestimate the contour length for the E[HH]$'_{i,j}$ species. For example, if extended stems II and III (E[HH]$'_{II,III}$) were coaxially stacked, with the entire core region looped out, the 159 bp control would overestimate the contour length by about 6%. This difference could account for nearly all of the observed reduction in $\tau_{II,III}$, leading to an estimated angle approaching 180°. However, the observed fractional amplitude (0.23) of the fast phase in the birefringence decay curve for E[HH]$'_{II,III}$ (Figure 4) is larger than that expected for the coaxial arrangement (0.10−0.13) and is consistent with a bend of 155−165° (Zacharias and Hagerman, unpublished experiments). A similar argument can be applied to the angles subtended by stems I and III (E[HH]$'_{I,III}$), and by stems I and II (E[HH]$'_{I,II}$); however, for these latter two constructs, foreshortening of the contour, with interhelix stacking, cannot account for all of the observed reductions in the τ's. Furthermore, the substantial fast amplitudes associated with the decay curves for these two species are consistent with subtended angles in the 100−120° range (Zacharias and Hagerman, unpublished experiments). The foregoing discussion probably overestimates the uncertainties associated with the contour lengths, since the helices cannot all be stacked simultaneously. Thus, the angles presented in Table 2 are probably reasonable estimates.

A second source of uncertainty is a potential pH dependence of the structure of the hammerhead core, since the electrophoretic and birefringence measurements have been restricted to pH values that are less than or equal to pH 7.0 (self-cleavage rates become too great for higher pH). However, we feel that a pH-dependent conformational change is unlikely, since there is no detectable alteration of the electrophoretic mobilities or the relative birefringence decay times between pH 6 and 7, even though the rate of self-cleavage increases by at least 100-fold over this pH range (no detectable cleavage at pH 6). In this regard, Dahm et al. (1993) have proposed that the pH dependence of the cleavage rate is a simple consequence of the titration of a magnesium hydrate, with the metal hydroxide being the active species in the cleavage reaction.

A third source of uncertainty is the possibility of increased flexibility of the core region. While this possibility cannot be ruled out at present, the significant asymmetry of the decay times for the three E[HH]$'_{i,j}$ species (Figure 4), the corresponding asymmetry in the electrophoretic mobilities, and a sum of the three angles near 360° all suggest that the core region possesses significant structural rigidity. Moreover, in preliminary measurements of the dependence of the E[HH] species on gel concentration, the relative mobilities of E[HH]$'_{I,III}$ and E[HH]$'_{I,II}$ are reduced by 1.5- and 1.9-fold, respectively, in going from 6% to 10% acrylamide, a result that is not expected for completely flexible nonhelical elements (Mills et al., 1994).

Finally, an adventitious widening of the interhelix angles due to repulsive electrostatic interactions between elongated stems is unlikely for the following reasons: (i) studies of four-way junctions with 115 bp extended arms yielded interhelix angles that were less than or equal to 60° (Cooper & Hagerman, 1989), much more acute than any of the angles observed in the current study; (ii) the apparent angles are insensitive to Mg^{2+} ion concentration in the 1−4 mM range, whereas reductions in all angles would be expected over this range if long-range repulsive interactions were important; (iii) in experiments with extended yeast $tRNA^{Phe}$ constructs in which the acceptor and anticodon stems have been extended with the same dsRNA arms employed in the current study, the observed interstem angles are slightly less than 90° (Friederich and Hagerman, in preparation), as expected from the crystal structure of yeast $tRNA^{Phe}$ (Holbrook et al., 1978); (iv) any interhelix distortions that are postulated to arise as a result of long-range repulsive (electrostatic or excluded volume) interactions would have to be compatible with a core conformation that is fully active in self-cleavage; (v) a computational analysis (Olmsted & Hagerman, 1994) of the extent of counterion association in the vicinity of branched nucleic acids suggests that, for the angles considered in the current work, the helix extensions would possess virtually no repulsive energy of interaction.

In our initial study of E[HH]$^s_{I,II}$ (Gast et al., 1994), we observed that the decay time of that species (3 bp stem III) was essentially identical to that of E[HH]$'_{I,II}$ (9 bp stem III). Since those measurements were performed to assess the direct hydrodynamic contribution of the short stem under conditions where cleavage was not occurring, they were performed in the absence of $MgCl_2$, although the buffer conditions were not reported. Therefore, the previous conclusion that elongation of stem III does not cause a significant structural rearrangement applies only to the (−) Mg^{2+} case. This latter point is important for the current

observations, because it suggests that a stable stem III and Mg^{2+} coordination within the hammerhead core are both required to form the fully-active conformer in solution.

The current investigation was designed to examine a specific aspect of RNA structure, namely, the influence of a nonhelical element (the hammerhead core) on the arrangement of adjacent helical stems. The hammerhead system represents a paradigm for study using the combined electrophoresis/birefringence approach, not only because of its small size, but also because self-cleavage represents a convenient assay for the formation of biologically-active structure. For the hammerhead system, the current approach has yielded both a specific global conformation for the hammerhead core and the observation that alterations in self-cleavage activity are accompanied by substantial alterations in global conformation. Finally, the current approach should be broadly applicable for the study of other elements of RNA structure (*e.g.*, internal loops, branches, etc.) in which a specific nonhelical element is flanked by well-defined helical stems.

ACKNOWLEDGMENT

The authors wish to thank Janine Mills for synthesizing the DNA oligomers, and for providing the parent plasmids used in this study. The authors would also like to thank Drs. Olke Uhlenbeck, Martin Zacharias, and Gregg Bellomy for useful discussions.

REFERENCES

Altman, S., Kirsebom, L., & Talbot, S. (1993) *FASEB J. 7,* 7−14.
Cech, T. R. (1990) *Annu. Rev. Biochem. 59,* 543−568.
Cooper, J. P., & Hagerman, P. J. (1987) *J. Mol. Biol. 198,* 711−719.
Cooper, J. P., & Hagerman, P. J. (1989) *Proc. Natl. Acad. Sci. U.S.A. 86,* 7336−7340.
Crothers, D. M., Haran, T. E., & Nadeau, J. C. (1990) *J. Biol. Chem. 265,* 7093−7096.
Dahm, S. C., Derrick, W. B., & Uhlenbeck, O. C. (1993) *Biochemistry 32,* 13040−13045.
Davies, C., Sheldon, C. C., & Symons, R. H. (1991) *Nucleic Acids Res. 19,* 1893−1898.
Fedor, M. J., & Uhlenbeck, O. C. (1992) *Biochemistry 31,* 12042−12054.
Forster, A. C., & Symons, R. H. (1987) *Cell 49,* 211−220.
Forster, A. C., Davies, C., Sheldon, C. C., Jeffries, A. C., & Symons, R. H. (1988) *Nature 334,* 265−267.
Gast, F.-U., & Hagerman, P. J. (1991) *Biochemistry 30,* 4268−4277.
Gast, F.-U., Amiri, K. M. A., & Hagerman, P. J. (1994) *Biochemistry 33,* 1788−1796.
Hagerman, P. J. (1990) *Annu. Rev. Biochem. 59,* 755−781.
Hagerman, P. J. (1992) *Biochim. Biophys. Acta 1131,* 125−132.
Hagerman, P. J., & Zimm, B. H. (1981) *Biopolymers 20,* 1481−1502.
Hertel, K., Herschlag, D., & Uhlenbeck, O. C. (1994) *Biochemistry 33,* 3374−3385.
Heus, H. A., & Pardi, A. (1991) *J. Mol. Biol. 217,* 113−124.
Heus, H. A., Uhlenbeck, O. C., & Pardi, A. (1990) *Nucleic Acids Res. 18,* 1103−1108.
Hodgson, R. A. J., Shirley, N. J., & Symons, R. H. (1994) *Nucleic Acids Res. 22,* 1620−1625.
Holbrook, S. R., Sussman, J. L., Warrant, R. W., & Kim, S.-H. (1978) *J. Mol. Biol. 123,* 631−660.
Hutchins, C. J., Rathjen, P. D., Forster, A. C., & Symons, R. H. (1986) *Nucleic Acids Res. 14,* 3627−3640.
Koizumi, M., & Ohtsuka, E. (1991) *Biochemistry 30,* 5145−5150.
Milligan, J. F., Groebe, D. R., Witherell, G. W., & Uhlenbeck, O. C. (1987) *Nucleic Acids. Res. 15,* 8783−8798.
Mills, J. B., Cooper, J. P., & Hagerman, P. J. (1994) *Biochemistry 33,* 1797−1803.
Odai, O., Kodama, H., Hiroaki, H., Sakata, T., Tanaka, T., & Uesugi, S. (1990) *Nucleic Acids Res. 18,* 5955−5960.
Olmsted, M. C., & Hagerman, P. J. (1994) *J. Mol. Biol.* (in press).
Pease, A. C., & Wemmer, D. E. (1990) *Biochemistry 29,* 9039−9046.
Press, W. H., Vetterling, W. T., Teukolsky, S. A., & Flannery, B. P. (1992) *Numerical Recipes in Fortran: The Art of Scientific Computing*, Cambridge University Press, pp 678−683, Cambridge, UK.
Provencher, S. W. (1982) *Comput. Phys. Commun. 27,* 229−242.
Robertson, H. D., & Branch, A. D. (1987) *The Viroid Replication Process*, in *Viroids and Viroid-like Pathogens* (Semanick, J. S., Ed.) pp 49−69, CRC Press, Boca Raton, FL.
Roitman, D. B. (1984) *J. Chem. Phys. 81,* 6356−6360.
Roitman, D. B., & Zimm, B. (1984a) *J. Chem. Phys. 81,* 6340−6347.
Roitman, D., & Zimm, B. H. (1984b) *J. Chem. Phys. 81,* 6348−6354.
Ruffner, D. E., Dahm, S. C., & Uhlenbeck, O. C. (1989) *Gene 82,* 31−41.
Shen, Z., & Hagerman, P. J. (1994) *J. Mol. Biol. 241,* 415−430.
Slim, G., & Gait, M. J. (1991) *Nucleic Acids Res.19,* 1183−1188.
Symons, R. H. (1989) *Trends Biochem. Sci. (Pers. Ed.) 14,* 445−450.
Symons, R. H. (1991) *Crit. Rev. Plant Sci. 10,* 189.
Symons, R. H. (1992) *Annu. Rev. Biochem. 61,* 641−671.
Uhlenbeck, O. C. (1987) *Nature 328,* 596−600.